SBrT 2019 1570556968

Airship's Antennas: Isolation analysis using simulation software tool

César Druczkoski, Cynthia C. M. Junqueira and Martin Vogel

***Abstract*— This paper shows, for a real-life airborne platform with multiple communication antennas, how simulation is used to evaluate possible electromagnetic interference problems. The simulations employ Altair's FEKO software with both its Method of Moments (MOM) and Multilevel Fast Multipole Method (MFLMM) solvers to validate the antenna models and their chosen location on a model airship. This approach ensures better project technical choices allowing cost reduction with manufacturing real prototypes and anechoic chamber tests.**

***Keywords*— FEKO, isolation, antennas, airship, EMI.**

I. Introduction

Antennas mounted in operational platforms, be it automobiles or aerospace vehicles, have inherent coupling and its effects need to be studied and well understood in order to avoid electromagnetic interference (EMI) among their systems. In a radio communication system project, antenna isolation is a key factor to be considered, especially when integrated in vehicles with different materials and of a significant size.

The antenna isolation is a measure of the power transfer from one antenna to the other in a transmitter and receiver system. The antenna isolation needs to be as large as possible to minimize interference effects and to allow each antenna to perform as intended. When systems work with low isolation, effects like intermodulation, receiver sensibility problems, transmitter noise, and adjacent channel interference can exist. There are several techniques to achieve this isolation, e.g., physical separation, polarization, optimization of radiation patterns and transmission coefficients.

The antenna characterization in a standalone condition is easy to perform using anechoic chambers, but when placed on large platforms the requirements for this anechoic chamber are not the same and factors like chamber size and costs are not negligible. So, the use of simulation software for wideband characterization of the installed antennas (giving a calculation of input impedance, radiation patterns, gain and the coupling between antennas) is essential. This approach allows gaining time in the development of the project and consequently lowering costs in the construction of prototypes on a real scale for later proof of concept, ensuring a quick and accurate response to the market.

César Druczkoski, Departamento de Processamento de Sinais e Comunicações (DSPCom), Faculdade de Engenharia Elétrica e de Computação, Universidade Estadual de Campinas, Campinas, SP, Brazil, e-mail: cmdcido@dca.fee.unicamp.br; Cynthia C. M. Junqueira, Departamento de Comunicações (DECOM), Faculdade de Engenharia Elétrica e de Computação, Universidade Estadual de Campinas, Campinas, SP, Brazil, e-mail: cynthiaj@decom.fee.unicamp.br; Martin Vogel, Altair Engineering, Hampton, VA, USA, e-mail: mvogel@altair.com.

In this work we will deal with a simplified version of a real airship, regarding its mechanical and envelope structure, as well the frequencies and type of antennas installed on it. The electromagnetic simulation tool used is FEKO 2018, more specifically, it's Method of Moments (MOM) and Multilevel Fast Multipole Method (MFLMM) solvers. This simulation is a means to validate the chosen location for the antennas and verify possible interfere between them, and thus support engineering decisions on project's challenges.

This work is divided in sections with section II describing the aircraft antenas and how the numerical modeling was done. Section III shows the individual antenna's simulation results. Section IV presents the antennas isolation analysis and section V finishes the work presenting a conclusion for this study.

II. Numerical modeling

The aircraft, antennas and communication system described in this work, although simplified, show a big similarity with an existing aircraft's structure [1]: a non-rigid airship which consists of a gondola mounted underneath a large helium balloon. The numerical modeling and simulation of the aircraft was done using the software tool Altair FEKO [2] which contains a 3D CAD tool and libraries of electrical and magnetic properties of dielectric and metallic materials.

In order to minimize errors and possible problems with the simplifications adopted, the modeling process was divided into: aircraft modeling; antenna modeling; simulation and characterization of the standalone antenna in free space; modeling of completed and simplified aircraft and antennas; simulation and characterization of each antenna, individually, in its respective location in the gondola (without the envelope); and simulation of all antennas integrated into it.

A. Aircraft modeling

The aircraft's structure model was simplified to minimize computational needs and speed up numerical simulations. The envelope, the aircraft's balloon, was considered uniform, without gores, welds or reinforcements and composed only by nylon (Nylon_610, FEKO Library [2]). Internal components, such as the ballonets and the internal catenaries, were also excluded. But here the helium filled envelope was not included due to computational resources available.

The gondola, where the antennas are located as seen in Fig. 1, was modeled with no internal component, no handling bars and no propeller, considered as a fiberglass shell (substrate_FR4, FEKO Library [2]) and the windows made of Plexiglas (plexiglass, FEKO Library [2]). The propeller hub

and the landing gear were modeled as stainless-steel structures (steel_stainless, FEKO Library [2]).

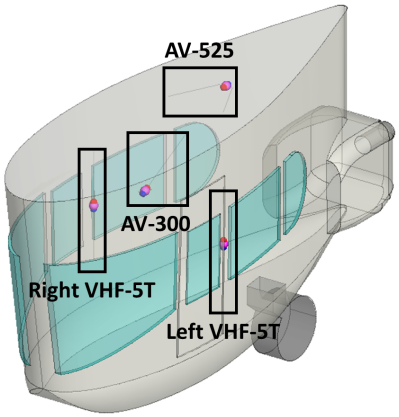

Fig. 1: Model of the gondola created in FEKO.

B. Antenna modeling

The antenna elements and communications systems installed on the aircraft are common off-the shelf components, similar to installations of many other Federal Aviation Regulations (FAR) part 23 [3] aircrafts [4], airships [5] and small helicopters [6]. To optimize available computational resources, the study was limited to the antennas with overlapping frequency bands, and so, more likely to suffer from poor isolation problems between them. Table I shows the chosen antennas and their electrical specifications, such as type, frequency and voltage standing wave ratio (VSWR).

TABLE I: Aircraft's antennas electrical specifications.

Antenna	Type	Frequency (MHz)	VSWR
VHF-5T	Half-wave dipole	108 to 136	1.6
AV-300	Whip monopole	121,5 and 406	2 and 1.5
AV-525	V dipole	108 to 118 and 329 to 335	3 and 2

1) VHF-5T antenna: The COMM VHF-5T antenna, as presented in its data sheet [7], is a half-wave dipole built on a fiberglass substrate (not specified) with approximate dimensions of 1092 x 25.4 x 0.635 mm, as shown in Fig. 2, and coated with an unspecified resin. This antenna has a balun for impedance matching. The antenna was modeled as a wire dipole with the approximate length of the actual antenna and a pi-match circuit optimized by the simulation software.

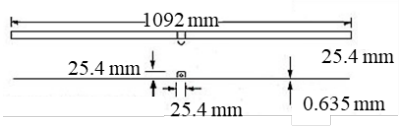

Fig. 2: VHF-5T antenna representation [7].

2) AV-300 antenna: The ELT AV-300 antenna, based on the manufacturer's data [8], Fig. 3, was modeled as a whip wire monopole and an angle between the base and the wire around 60°. The base of the antenna was simulated as a rectangle of a perfect electric conductor (PEC), from FEKO Library [2] with its dimensions optimized to be close the original one. The impedance matching was made with a pi-match circuit.

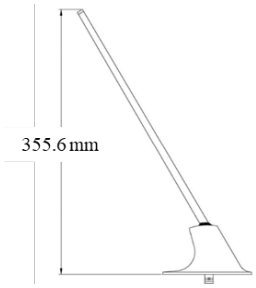

Fig. 3: AV-300 antenna representation [8].

3) AV-525 antenna: Based on [9], the VOR/LOC/GS AV-525 antenna is a V dipole with an aperture of approximately 120°, Fig. 4, with a balun for impedance matching. For modeling, the antenna has been simplified to a wire V dipole. A software optimized pi-match circuit was integrated into the antenna, but its effect was not significant.

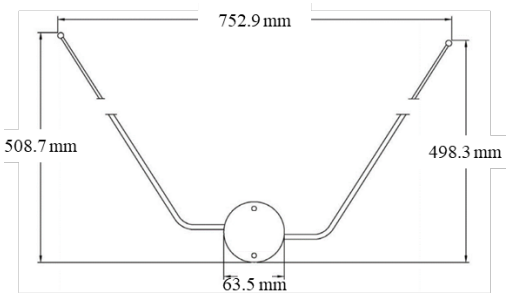

Fig. 4: AV-525 antenna representation [9].

III. Numerical simulation results

The antennas were simulated, using MOM solver, individually in the free space. When placed inside the gondola, MOM and MFLMM solvers were used. These results are shown for each antenna, Fig. 5 to Fig. 10, with the Left VHF-5T and the Right VHF-5T shown as only one simulation due to the symmetry of the airship's model on its longitudinal axis.

A. VHF-5T antenna results

As expected, the simulated VHF-5T antenna's radiation pattern in free space was compatible with the patterns of a half-wave dipole antenna [10]. Fig. 5 shows the Left VHF-5T antenna's radiation pattern inside the aircraft's gondola. The structure caused some deformation in the radiation pattern, flattening it, generating little valleys and peaks, causing a slight decrease in total gain around 1 dBi and resulting in a beamwidth of approximately 63° at $\phi = 90°$ (a 15° decrease when compared to freespace).

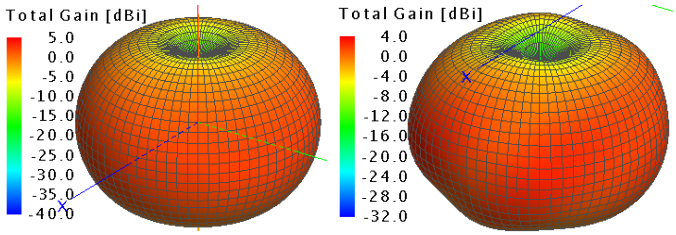

(a) In free space (b) Inside gondola

Fig. 5: VHF-5T 3D model radiation pattern (120MHz).

Fig. 6 compares the curve of the magnitudes of the VHF-5T antenna model's reflection coefficient ($|S_{11}|$) on free space and located inside the aircraft's gondola. As shown, the difference caused by the antenna positioning in the gondola is not significant. The values of VSWR are smaller than 2 in the band of 116 to 124 MHz in both scenarios.

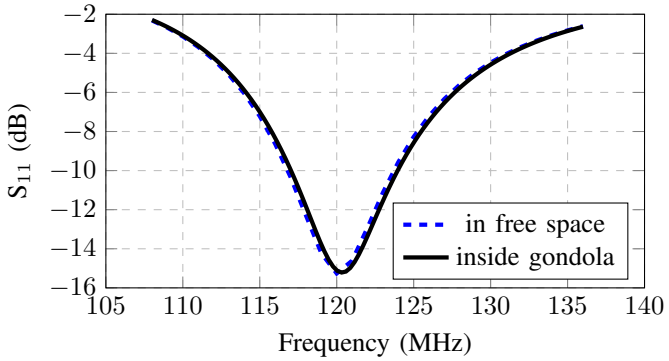

Fig. 6: VHF-5T antenna model's $|S_{11}|$.

B. AV-300 antenna results

The simulated AV-300 antenna's radiation pattern in free space was compatible with the patterns of a monopole whip antenna [10]. Fig. 7 shows the AV-300 antenna's radiation pattern located inside the aircraft's gondola. The gondola's structure caused a deformation in the radiation pattern of the antenna generating valleys and peaks on the toroidal diagram and resulting in a beamwidth of approximately 79° at $\phi = 90°$ (a 3° decrease when compared to freespace).

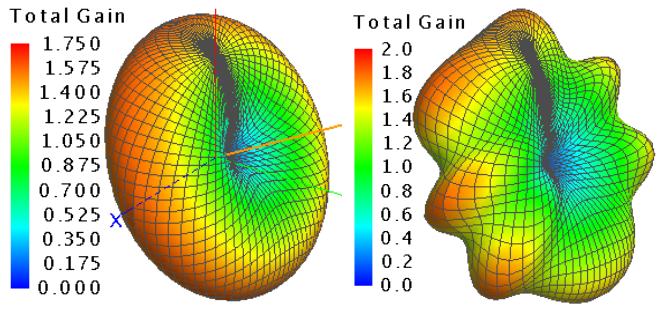

(a) In free space (b) Inside gondola

Fig. 7: AV-300 3D model radiation pattern (121.5 MHz).

Fig. 8 compares the AV-300 antenna model's $|S_{11}|$ on free space and inside the aircraft's gondola. As shown, the modeled structure worsens the $|S_{11}|$ by 1 dB. The VSWR are around 2.2 from 121.5 to 122.4 and 1.53 from 405 and 406 MHz.

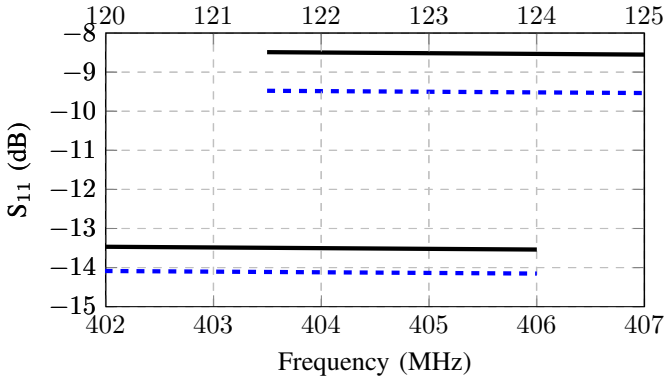

Fig. 8: AV-300 antenna model's $|S_{11}|$.

C. AV-525 antenna results

The AV-525 antenna's radiation pattern located inside the gondola are shown in Fig. 9. The pattern in free space was compatible with the diagrams of a V dipole antenna [10]. As can be seen the gondola structure causes a deformation in the radiation pattern generating 0.75 dBi variation and resulting in a beamwidth of approximately 107° at $\phi = 90°$ (a 1° decrease when compared to freespace).

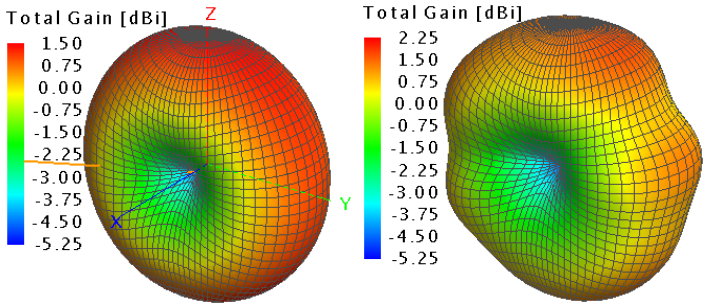

(a) In free space (b) Inside gondola

Fig. 9: AV-525 3D model radiation pattern (109 MHz).

Fig. 10 compares the AV-525 antenna model's $|S_{11}|$ in free space and inside the aircraft's gondola. The results from the antenna mode are similar to the real antenna [9] between 109 and 116 MHz band with a VSWR < 3. But in its second band, between 329 and 335 MHz, the simulated model does not reach the datasheet value of VSWR < 2 [9].

IV. Isolation: Results and Analysis

As stated, given the limitations of the hardware used, the necessary simplifications done in the aircraft model and some mismatching problem in one of the simulated antennas located at the aircraft impose some constraints on the complete analysis but will not significantly alter the results.

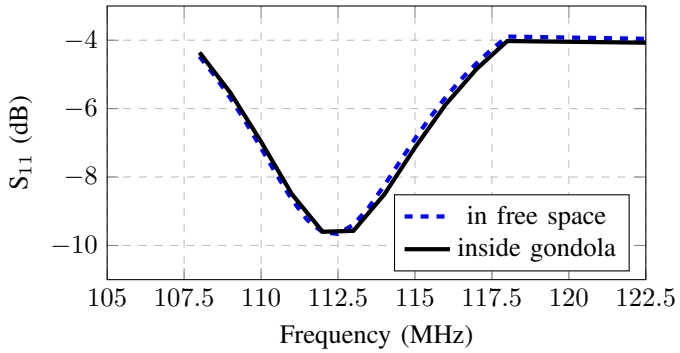

(a) 108 to 118 MHz range

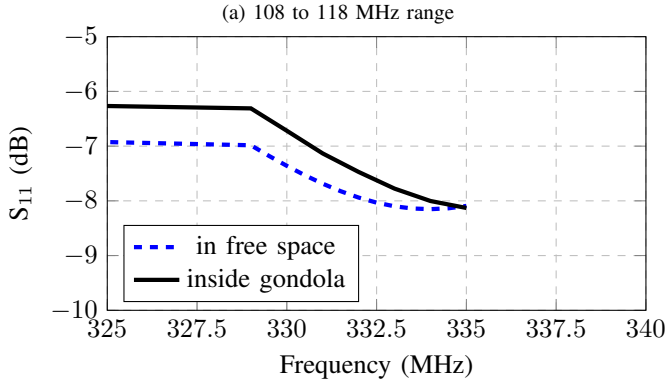

(b) 329 to 335 MHz range

Fig. 10: AV-525 antenna model's $|S_{11}|$.

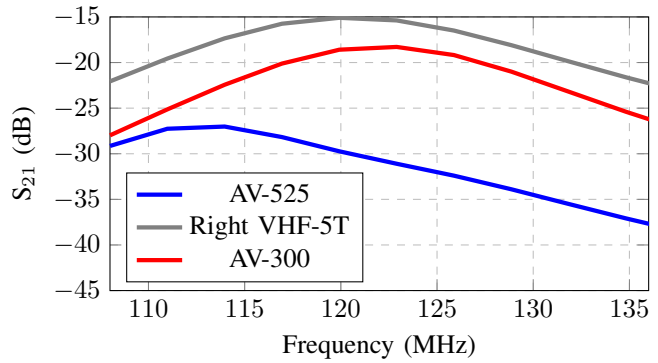

(a) 108 to 136 MHz range

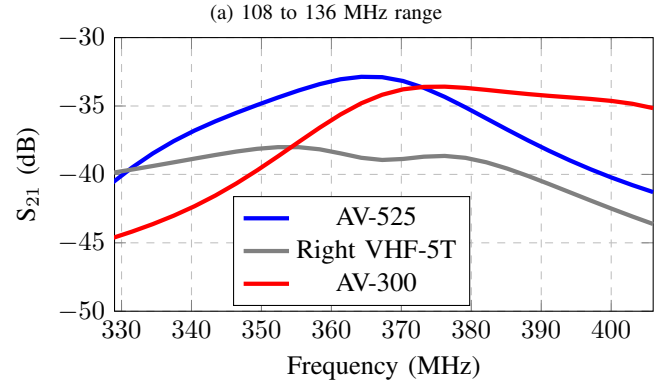

(b) 329 to 406 MHirship's antenna isolation: analysis using simulation software toolz range

Fig. 11: Left VHF-5T antenna model's $|S_{21}|$.

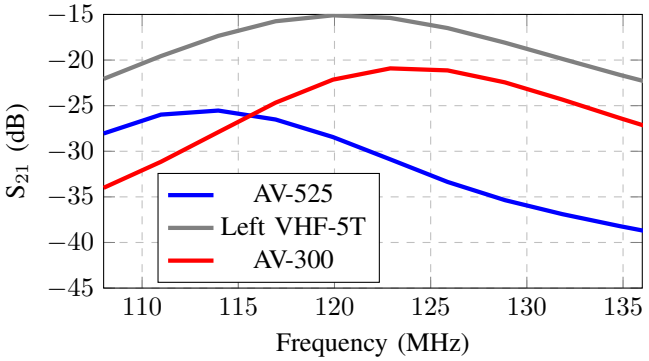

(a) 108 to 136 MHz range

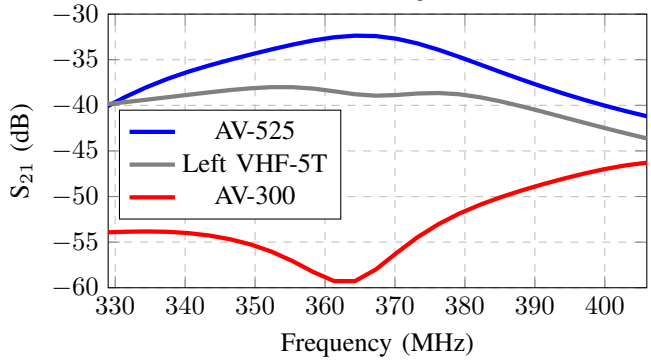

(b) 329 to 406 MHz range

Fig. 12: Right VHF-5T antenna model's $|S_{21}|$.

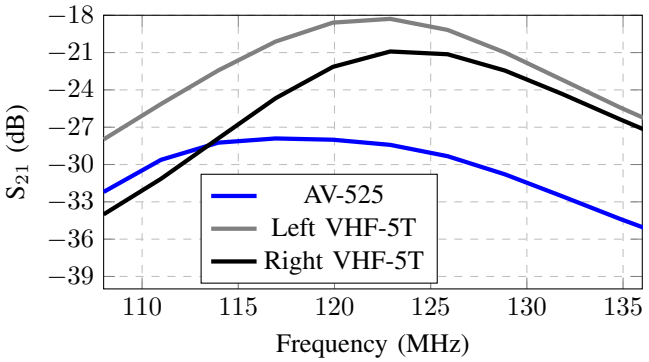

(a) 108 to 136 MHz range

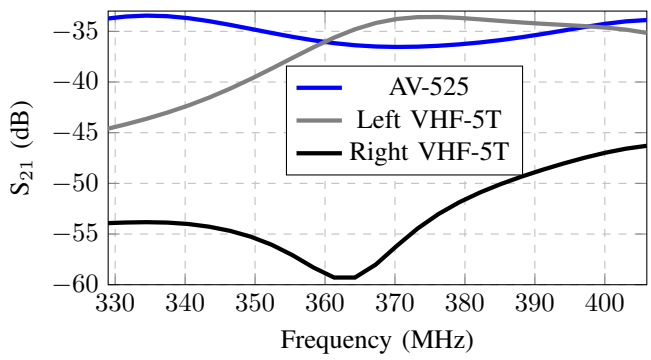

(b) 329 to 406 MHz range

Fig. 13: AV-300 antenna model's $|S_{21}|$.

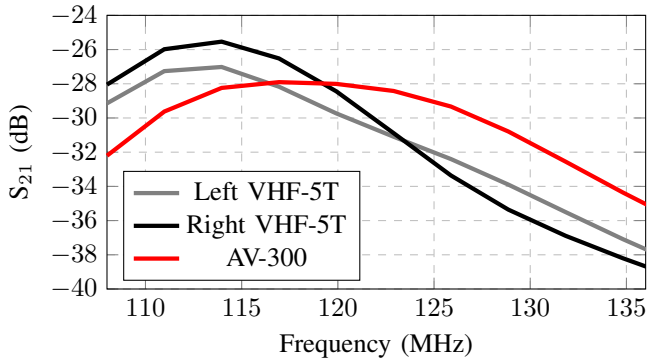

(a) 108 to 136 MHz range

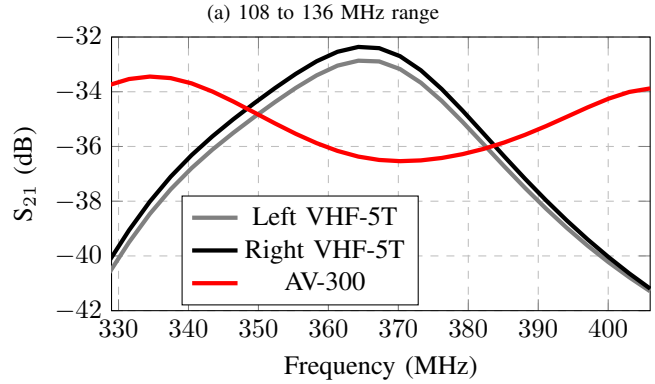

(b) 329 to 406 MHz range

Fig. 14: AV-525 antenna model's $|S_{21}|$.

Above, we present the magnitudes of the transmission coefficient ($|S_{21}|$), which indicate the isolation between the antennas versus frequency band for each pair of antenna. The curves shown in Fig. 11 are for the Left VHF-5T antenna, in Fig. 12 for the Right VHF-5T antenna, in Fig. 13 for the AV-300 antenna and in Fig. 14 for the AV-525 antenna.

Note from Fig. 11 that the worst isolation occurs between Right VHF 5T and Left VHF-5T, as expected, because they are exactly in same frequency range. The isolation values exceed -20dB between 115 and 132 MHz. When compared with AV-300 we see the same isolation level in the band 116 to 128 MHz. Better isolation values are found when compared with AV-525, where the worst isolation is -27dB. In the Fig. 11, no isolation problems are seen ($|S_{21}| <$ -32 dB).

The isolation of AV-300 antenna between 108 and 136 MHz presents worst values than in the range of 329 to 406 MHz, mainly with the antenna Left VHF-5T. This behavior was already expected, since the four antennas in this study operate in the first range while only two of them operate on the second.

From the similarity of curves of the two VHF-5T antennas we see that given the proximity of the AV-300 antenna to the antenna located on the left, it ends up having a lower isolation to the AV-300 antenna than to the one on the right side of the gondola has. This fact is also seen on the AV-300 antenna, being its smallest isolation for the nearest antenna.

V. Conclusions

Due to the simplifications made on the study and the meager information available on each of the commercial antennas, such as construction details and radiation pattern, the modeled antennas do not show exactly the same performance described in Table I, but the similarities justify the approximations made. The simplified gondola's structure also ends up furthering the gap between the results presented and those we would find in a real operating condition. This, however, does not disregards the acquired data and the conclusion that studied installation has an overall good isolation between its antennas.

Therefore, the use of electromagnetic simulation software, even with simplified models, can serve as a very good tool that speeds up the process of evaluating possible electromagnetic interference and installation problems prior to a prototype phase, thus reducing both costs and project time. This fact is even more significant for complex projects, with a lot of communication systems and possible sources of interference, where results and good practices may not be sufficient to guide the studies, and so, simulations, even if they take days, can save months of redesign and high costs.

Acknowledgments

We thank Gopinath Gampala and Aseim Elfrgani, Altair's Application Engineers, for all support given during the development and simulation of aircraft models.

References

[1] M. H. Hamley, "US LTA 138S airship as an airborne research platform", *Proceedings of the First International Airborne Remote Sensing Conference and Exhibition*, pp. 341–350, 1994.

[2] Altair Engineering SA., *Feko*, version 2018. [Online]. Available: https://altairhyperworks.com/product/FEKO.

[3] Federal Aviation Administration, *Part 23 - airworthiness standards: Normal category airplanes*.

[4] Hawker Beechcraft Corporation, *Model G58 baron pilot's operating handbook and faa approved airplane flight manual*, http://beechcraft.com/customer_support/technical_publications/docs/technical/58-590000-67_Main_Menu.htm.

[5] Zeppelin Luftschifftechnik, *Technology Zeppelin – NT am Bodensee*, https://zeppelin-nt.de/en/zeppelin-NT/technology.html.

[6] Power Helicópteros, *B2 PW003 Preto_Tan*, https://pt.scribd.com/document/356918149/B2-PW003-Preto-Tan.

[7] Advanced Aircraft Electronics Inc., *AAE_VHF_COM_NAV_Antenna.pdf*, http://www.carefreemaneuver.com/traveller/documents/AAE_VHF_COM_NAV_Antenna.pdf.

[8] RAMI, *RAMI | AV-300*, http://www.rami.com/product/av-300/.

[9] ——, *RAMI | AV-525*, http://www.rami.com/product/av-525/.

[10] R. C. Johnson and H. Jasik, *Antenna Engineering Handbook*, 3rd ed. McGraw Hill, Inc., Jun. 1993.